Carbohydrate Polymers 154 (2016) 139–150

Contents lists available at ScienceDirect

Carbohydrate Polymers

journal homepage: www.elsevier.com/locate/carbpol

Novel sulfated xylogalactoarabinans from green seaweed *Cladophora falklandica*: Chemical structure and action on the fibrin network

Paula X. Arata[a], Irene Quintana[b], María Paula Raffo[c], Marina Ciancia[a,d,*,1]

[a] Universidad de Buenos Aires, Facultad de Agronomía, Departamento de Biología Aplicada y Alimentos, Cátedra de Química de Biomoléculas, Av. San Martín 4453, C1417DSE Buenos Aires, Argentina
[b] Universidad de Buenos Aires, Facultad de Ciencias Exactas y Naturales, Departamento de Química Biológica, Laboratorio de Hemostasia y Trombosis, Ciudad Universitaria – Pabellón 2, C1428EHA Buenos Aires, Argentina
[c] Consejo Nacional de Investigaciones Cientificas y Tecnicas-Centro Nacional Patagónico (CENPAT-CONICET), Bvd. Brown 2915, U9120ACD Puerto Madryn, Chubut, Argentina
[d] Universidad de Buenos Aires, Facultad de Ciencias Exactas y Naturales, Departamento de Química Orgánica, Consejo Nacional de Investigaciones Cientificas y Tecnicas-Centro de Investigación de Hidratos de Carbono (CIHIDECAR-CONICET), Ciudad Universitaria – Pabellón 2, C1428EHA Buenos Aires, Argentina

ARTICLE INFO

Article history:
Received 27 June 2016
Received in revised form 11 July 2016
Accepted 20 July 2016
Available online 21 July 2016

Keywords:
Sulfated arabinan
Galactofuranose
Green seaweed
Cladophora
Anticoagulant activity
Fibrin network

ABSTRACT

The water-soluble sulfated xylogalactoarabinans from green seaweed *Cladophora falklandica* are constituted by a backbone of 4-linked β-L-arabinopyranose units partially sulfated mainly on C3 and also on C2. Besides, partial glycosylation mostly on C2 with single stubs of β-D-xylopyranose, or single stubs of β-D-galactofuranose or short chains comprising (1 → 5)- and/or (1 → 6)-linkages, was also found. These compounds showed anticoagulant activity, although much lower than that of heparin. The effect of a purified fraction (F1) on the fibrin network was studied in detail. It modifies the kinetics of fibrin formation, suggesting an impaired polymerization process. Scanning electron microscopy showed a laxer conformation, with larger interstitial pores than the control. Accordingly, this network was lysed more easily. These fibrin properties would reduce the time of permanence of the clot in the blood vessel, inducing a lesser thrombogenic state. One of the possible mechanisms of its anticoagulant effect is direct thrombin inhibition.

1. Introduction

Cladophora Kützing is one of the largest green algal genera and has a worldwide distribution. Within the class Cladophorophyceae, the genus *Cladophora* is characterized by its simple thallus architecture: branched, uniseriate filaments of multinucleate cells. *Cladophora* cell walls, which are several micrometers thick, were reported to consist largely of cellulose, which represents about 15% of the biomass (Wissel, Mayr, & Lücke, 2008).

In spite of its wide distribution, which comprises mostly marine, but also fresh water environments, and of its abundance, there is only scarce information about the structure of the sulfated polysaccharides biosynthesized by algae of this genus. Percival and coworkers studied the structural features of the water soluble polysaccharides from *Cladophora rupestris* (Percival & McDowell, 1981). These studies established the presence of arabinose, galactose, xylose, rhamnose, and glucose in the approximate molar proportions of 3.7:2.8:1.0:0.4:0.2 (+8% protein) and 19.6% half ester sulfate. Application of degradative studies provided evidence of a highly branched structure, with xylose and galactose units at the ends of the branches and galactose, arabinose, and rhamnose residues occurring in the inner part of the molecules. Evidence of 6-linked and/or 6-sulfated galactofuranose units was obtained. Partial hydrolysis experiments led to the separation and characterization of the following fragments: L-arabinose 3-sulfate, D-galactose 6-sulfate, 3-linked and 6-linked D-galactobioses, 4- or 5-linked L-arabinobiose 3-sulfate, 4-linked D-xylobiose, a mixture of trisaccharides containing sulfated galactose and arabinose, and a mixture of pentasaccharides in which the molar ratio of arabinose to galactose was 4:1.

Later, the structural characteristics of the polysaccharides obtained from *Cladophora socialis* by extraction with dilute acid were reported (Sri Ramana & Venkata Rao, 1991). A molar ratio

* Corresponding author at: Cátedra de Química de Biomoléculas, Departamento de Biología Aplicada y Alimentos, Facultad de Agronomía, Universidad de Buenos Aires, Av. San Martín 4453, C1417DSE Buenos Aires, Argentina.
E-mail address: ciancia@agro.uba.ar (M. Ciancia).
[1] Research Member of the National Research Council of Argentina (CONICET).

http://dx.doi.org/10.1016/j.carbpol.2016.07.088
0144-8617/

galactose:arabinose:xylose of 4.5:3.0:1.0 and 16.9% of sulfate were determined. Similar conclusions were obtained regards the arabinose units, but no galactose in the furanose form was detected. In this case, galactose units were found to be 3-linked and sulfated on C4 or C4 and C6.

Between the sulfated polysaccharides, sulfated fucans (SFs) and sulfated galactans (SGs) are currently the marine non-glycosaminoglycan (GAG) sulfated compounds most studied in glycomics. These polysaccharides exhibit therapeutic effects in several pathophysiological systems such as blood coagulation, thrombosis, neovascularization, cancer, inflammation, and microbial infections. As analogs of the largely employed GAGs and due to some limitations of the GAG-based therapies (Anand, Yusuf, Pogue, Ginsberg, & Hirsh, 2003; Kelton & Hirsh, 1980; Kelton & Warkentin, 2008), SFs and SGs comprise new carbohydrate-based therapeutics available for clinical studies. However, the degree and mechanism of action varies greatly, not only with the degree of sulfation, but also with their chemical structure, and other sulfated polysaccharides with different carbohydrate backbones and sulfate distributions have been investigated and were found to have similar properties (Ciancia, Quinitana, & Cerezo, 2010, Fernández et al., 2013).

In a previous paper, the effect in the fibrin network formation of sulfated galactans from green seaweeds of the order Bryopsidales was studied by measuring optical density (OD) at 405 nm *vs* time. It was shown that these galactans caused an impaired assembly of fibrin monomers into the fibrin polymer (Arata et al., 2015).

Kinetics of fibrin formation gives a different insight into the study of the coagulation process, contributing to the understanding of the mechanism of anticoagulant activity. On the other hand, the study of fibrinolysis is also crucial, because currently approved thrombolytic drugs have side effects, such as bleeding, low specificity on account of being indirect plasminogen activators, and high cost. The 'holy grail' for antithrombotic therapy, a drug that prevents coagulation without promoting bleeding, has yet to be found.

In this paper, structure of the major water-soluble sulfated polysaccharides from *Cladophora falklandica* was determined, and their anticoagulant effect was investigated, not only by general coagulation tests, but also through studies of their influence in fibrin formation and fibrinolysis. Besides, characteristics of the fibrin clot were examined using scanning electron microscopy.

2. Experimental

2.1. Algal sample

Specimens of *Cladophora falklandica* (J.D. Hooker & Harvey) J.D. Hooker & Harvey were collected in Punta Este – Puerto Madryn – Chubut – Argentina (42°46′48″S, 64°57′W), in September 2010. The samples used in this work were in the vegetative state. Thalli of the seaweeds were washed with sea water and analyzed for epiphytic and epizoic contaminants in a Nikon AFX-II macroscope (Nikon, Japan). Voucher specimens were deposited in the Museum Bernandino Rivadavia, Buenos Aires Argentina (collection code: BA: 47426).

2.2. Extraction of the polysaccharides

Algal samples of *C. falklandica* were dried in open air. The extraction procedure was described elsewhere (Ciancia et al., 2007). Briefly, the milled seaweds (100 g) were extracted twice with EtOH 70% (20 g/L) for 3 h at room temperature. The residue from the alcohol extraction was extracted with H2O (20 g/L) at room temperature for 18 h giving a product, which was recovered from the supernatant by dialysis and freeze dried (extract CX1). The residue from the first H_2O extraction was extracted twice more in similar conditions to give extracts CX2 and CX3. The residue from the room temperature H_2O extraction was extracted three times for 3 h with H_2O (20 g/L) at 90 °C, giving extracts CC1–CC3.

2.3. Ion exchange chromatography (IEC)

CX2 was chromatographed on DEAE-Sephadex A-25. The sample (220 mg) was dissolved in water (30 mL), centrifuged, and the supernatant was applied to a column (90 × 1.5 cm id), previously stabilized in H_2O. The first elution solvent was water, and then NaCl solutions of increasing concentration up to 4 M. Fractions of 4 mL were collected. Finally, the phase was boiled in 4 M NaCl solution. The presence of carbohydrates in the samples was detected by the phenol – sulfuric acid method (Dubois, Gilles, Hamilton, Rebers, & Smith, 1956); after obtaining blank readings, the eluant was replaced by another with higher concentration of NaCl. Eleven fractions were obtained, dialyzed and freeze dried (F1–F11).

2.4. Chemical analyses

The total sugars content was analyzed by the phenol-sulfuric acid method (Dubois et al., 1956). Sulfate was determined turbidimetrically (Dodgson & Price, 1962). Alternatively, ion exchange chromatography with conductimetric detection was used: the sample was hydrolyzed in 2 M CF3CO2H at 121 °C for 2 h, evaporated to dryness under nitrogen and redissolved in high purity water from a Milli-Q system. A DIONEX DX-100 chromatography system (Sunnyvale CA, USA) was used with an AS4A column (4 × 250 mm), an AMMS-II micromembrane suppressor and a conductivity detector, elution was carried out with 1.8 mM Na_2CO_3/1.7 mM $NaHCO_3$, at a flow rate of 2 mL min^{-1}. The absence of pyruvic acid and uronic acids was confirmed using the colorimetric determinations of Koepsell and Sharpe (1952) and Filisetti-Cozzi and Carpita (1991), respectively. The protein content was measured by the method of Bradford (1976) (BioRad protein assay), Lowry, Rosenbrough and Farr (1951), and using a kit Pierce™ BCA Protein Assay Kit; however, results were very variable, so microanalysis was performed to determine the amount of nitrogen, a factor of 5 was applied to calculate the amount of protein, according to Angell, Mata, de Nys and Paul (2016). The configuration of galactose and arabinose was determined by the method of Cases, Cerezo and Stortz (1995) through their diastereomeric acetylated 1-deoxy-1-(2-hydroxypropylamino) alditols. To determine the monosaccharide composition, samples were derivatized to the alditol acetates (Stevenson & Furneaux, 1991). Number average molecular weight of CX2 and F1 was estimated by the method of Park and Johnson (1949). Dialyses were carried out with tubing with molecular weight cutoff of 3500 Da.

2.5. Desulfation of F1 and CC2

The reaction was carried out by the microwave-assisted method described by Navarro, Flores and Stortz (2007). The sample (40 mg) was converted to the pyridinium salt and dissolved in 10 mL of DMSO containing 2% of pyridine. The mixture was heated for 10 s intervals and cooled to 50 °C (×6). It was dyalized 3 days against tap water and then 24 h against distilled water and lyofilized. An aliquot was methylated as described bellow without previous isolation of the product.

2.6. Partial acid hydrolysis of F1

The reaction was carried out according to Bilan, Vinogradova, Shashkov, and Usov (2007). The sample (50 mg) was heated in 1%

CH_3COOH (10 mL) for 4 h at 100 °C, the solution was neutralized with $NaHCO_3$, dialyzed, and lyophilized to give F1H (21.5 mg).

2.7. Methylation analysis

The sample (10–20 mg) was converted into the corresponding triethylammonium salt (Stevenson & Furneaux, 1991) and methylated according to Ciucanu and Kerek (1984). The sample was dissolved in dimethylsulfoxide; finely powdered NaOH was used as base. For F1, different times between addition of the base and of CH_3I were assayed and also two sequential methylation steps were tested. However, in the latter case, labile sugars where lost, so only one methylation step was used. The methylated samples were submitted to reductive hydrolysis and acetylation to give the alditol acetates in the same way as the parent polysaccharides (Stevenson & Furneaux, 1991). Derivatization of the permethylated samples in the standard conditions (Morrison, 1988) showed partial degradation, so results obtained by this method were not considered.

2.8. Gas chromatography

GC of the alditol acetates were carried out on a Agilent 7890A gas-liquid chromatograph (Avondale PA, USA) equipped with a flame ionization detector and fitted with a fused silica column (0.25 mm i.d. x 30 m) WCOT-coated with a 0.20 μm film of SP-2330 (Supelco, Bellefonte PA, USA). Chromatography was performed: from 200 °C to 240 °C at 2 °C min^{-1}, followed by a 10-min hold for alditol acetates. For the partially methylated alditol acetates, the initial temperature was 160 °C, which was increased at 1 °C min^{-1} to 210 °C and then at 2 °C min^{-1} to 230 °C. N_2 was used as the carrier gas at a flow rate of 1 mL min^{-1} and the split ratio was 80:1. The injector and detector temperature was 250 °C.

2.9. GC–MS

GC–MS of the methylated alditol acetates was performed on a Agilent 7890A gas-liquid chromatograph equipped the SP-2330 interfaced to a Agilent 5977A Series mass spectrometer, working at 70 eV. He flow rate was 1.3 mL min^{-1}, the injector temperature was 250 °C. Mass spectra were recorded over a mass range of 30–500 amu.

2.10. NMR spectroscopy

500 MHz ^1H NMR, proton decoupled 125 MHz ^{13}C NMR spectra, and two-dimensional NMR experiments (HSQC, HMBC, and COSY) were recorded on a Bruker AM500 at room temperature, with external reference of TMS. The samples (20 mg) were exchanged in 99.9% D2O (0.5 mL) four times. Chemical shifts were referenced to internal acetone (δ_H 2.175, δ_{CH3} 31.1). Parameters for ^{13}C NMR spectra were as follows: pulse angle 51.4°, acquisition time 0.56 s, relaxation delay 0.6 s, spectral width 29.4 kHz, and scans 25,000. For ^1H NMR spectra: pulse angle 76°, acquisition time 3 s, relaxation delay 3 s, spectral width 6250 Hz and scans 32. 2D spectra were obtained using standard Bruker software.

2.11. General coagulation assays

The tests were performed with a coagulometer ST4 (Diagnostica Stago, Asnieres sur Seine, France). Determinations of prothrombin time (PT), activated partial thromboplastin time (APTT), and thrombin time (TT) were assayed according to established methods (Laffan & Bradshaw, 1995). Reagents were supplied by Diagnostica Stago, except tromboplastin reagent. Since polybrene, a known neutralizer of heparin, is added to the majority of the PT commercial reagents tromboplastin was extracted from rabbit brain according to the method described by Quick (1935). Normal platelet depleted citrated plasma (900 μL) was mixed with 100 μL of the polysaccharide sample, in different concentrations (5–100 μg/mL), and incubated for 1 min at 37 °C. Heparin (Sigma, St. Louis, MO, USA) and dermatan sulfate (Syntex, Buenos Aires, Argentina) were used for the comparison of anticoagulant activity of the fractions. Saline solution (0.9% NaCl) was used as control. TT-like assays were also performed with purified fibrinogen (Sigma, St. Louis, MO, USA) (3 mg/mL) instead of human plasma. All clotting assays were performed in quadruplicate. Results were expressed as ratios between clotting time of a solution of the anticoagulant and clotting time of the control.

2.12. Formation and evaluation of fibrin networks

A pool of normal citrated plasma (platelet depleted) was mixed with each of the polysaccharides samples (5–100 μg/mL) in a ratio 9:1. Similar assays were also performed with purified fibrinogen (1 mg/mL) instead of plasma. Assays were carried out in quadruplicate in polystyrene strips, using saline solution as control. Fibrin generation and fibrin networks were evaluated by kinetic assays and scanning electronic microscopy, respectively.

2.12.1. Kinetic assays

Clots were generated by adding thrombin (0.5 IU/mL) to plasma. Fibrin formation kinetics was evaluated by measuring optical density (OD) at 405 nm, every 1 min until constant values were reached (ELx808, BioTek Instruments Inc., Winooski, VT, USA). The curves obtained (OD_{405} vs. time) were characterized by three parameters: the *lag phase*, which reflects the time required for initial protofibril formation; *the slope*, which corresponds to the maximum velocity achieved (V_{Max}) and the *final network OD* (OD_{Max}) at the plateau phase, which is influenced by the number of protofibrils per fiber (Wolberg, Gabriel & Hoffman, 2002).

2.12.2. Scanning electron microscopy (SEM)

Incubated plasma in the presence of F1 at a final concentration of 5, 15, and 25 μg/mL and controls were obtained as described above, using little pieces of glass as support. Gels were stabilized in a moist camera 2 h at room temperature and fixed in glutaraldehyde 2% overnight. After being washed, they were dehydrated in graded ethanol-water solutions (50–100%), dried by critical point procedure (EMS 850 Critical Point, Hatfield, PA, USA) and gold-palladium coated (Polaron Thermo VG Scientific SC 7620, West Sussex, England). Observations were carried out in a scanning electron microscope (Carl Zeiss DMS 940A, Oberkochen, Germany) at 5 kV. Photographs were obtained at a magnification of 10.000 X. Quantitative analysis of fibrin networks in the respective photographs was performed using ImageJ 1.48v software (National Institutes of Health, USA). 10 randomly selected fields of the same area were evaluated, and each network was characterized by number of fibers per field, network percentage (ratio between total surface of the fibers and total field area x100), width and length of the fibers.

2.13. Lysability assays

Lysis was performed in a one-stage assay by adding tPA (25 IU/mL) to a pool of preincubated normal citrated plasma (platelet depleted) at the same time as thrombin (0.5 IU/mL). The concentrations used were chosen to achieve maximum polymerization of the network. The plasma was mixed with each of the polysaccharides samples in a ratio 9:1. Kinetics parameters were obtained by measuring optical density at 405 nm vs. time during 3 h. Assays were performed by quadruplicated and results were expressed in terms

of *half-lysis-time* ($t_{1/2}$) as the time in which the turbidity of the clot is reduced to its half-maximal value.

2.14. Statistical analysis

Data from anticoagulant activity assays were analyzed using the statistical software *Statistix 8* (Analytical Software, Tallahassee, FL, USA). According to the case, results were expressed as mean ± standard deviation, or median (range). Student's *t*-test or method of Mann–Witney–Wilcoxon was used to compare the results and p values < 0.05 where considered statistically significant.

3. Results and discussion

3.1. Extraction and characterization of the sulfated polysaccharides

Water-soluble polysaccharides from green seaweed *Cladophora falklandica* were obtained by sequential extraction at room temperature and at 90 °C from the alcohol insoluble residue, giving a total yield of 29.2% of the dry milled material.

All the extracts have important amounts of carbohydrates and sulfate (Supplementary Table 1). Colorimetric assays indicated only trace amounts of uronic acids and no pyruvic acid ketals in these extracts, which have the same monosaccharides, but in different amounts. CX2 and CC2 were chosen for further studies (Table 1). CX2 gave the highest yield, also, the highest amount of arabinose, and no glucose. Enantiomeric analysis of this sample showed that galactose is in the D-configuration, while arabinose belongs only to the L-series. The protein content of this extract is 6.5%. Determination of molecular weight by the colorimetric method of Park and Johnson (1949) indicated a molecular weight of 19 KDa.

3.2. Fractionation of CX2 and structural study of the major fractions

CX2 was fractionated by anion exchange chromatography on Sephadex A-25. Table 1 shows the yields and analyses of the fractions isolated in the highest amounts.

The major fraction, F1, eluted with water, in spite of the fact that it has a significant percentage of sulfate. Its monosaccharide composition is similar to that of the parent sample. The molar ratio Ara:Xyl:Gal:sulfate was 1.0:0.2:0.4:0.8. Structural analysis was carried out on F1 by methylation, desulfation-methylation, and partial hydrolysis-methylation procedures (Table 2), and the original sample, as well as its derivatives were analyzed by NMR spectroscopy.

Results from methylation analysis and ^{13}C NMR spectra of F1, as well as of its desulfated derivative (F1D) are shown in Table 3 and Fig. 1a. ^{13}C NMR spectrum of F1 shows three groups of signals in the anomeric region, namely, a major one at $\delta \sim 97$–98, another at $\delta \sim 108$–110, which desappeared in the spectrum of F1D, and a minor one at $\delta \sim 105.5$–106. Table 3 shows the presence of 2,3,5,6-tetra-*O*-methyl- and 2,3,5-tri-*O*-methyl-galatose between the partially methylated derivatives obtained from F1, indicating that at least part of the galactose units are in the furanose form. These furanosic galactose units were present only in minor amounts in F1D, indicating that they were lost during the desulfation procedure. Analysis of the experimental method suggested that hydrolysis of some galactofuranose units could take place during preparation of the sample, which comprises formation of the pyridinium salt. The resulting solution had a pH of 3.5. Although this solution was immediatelly neutralized with pyridine, the high lability of the furanosic glycosidic linkages would be enough to cause a certain degree of hydrolysis, even at room temperature. This result was confirmed by analysis of the monosaccharide composition of the desulfated derivative, which showed a decrease in galactose content from 22.3 to 12.0%, the diversity of the remaining galactose structural units could be the reason for the absence of these signals in the NMR spectra. Galactose detected in F1D could derive, in part, from small amounts of structures, in which this monosaccharide is in the pyranose form (see later).

The anomeric region of the HSQC spectrum of F1D (Fig. 1b) showed one major signal at δ 97.4/5.03, and two minor ones at δ 98.1/5.18 and 105.8/4.46, the first two signals were assigned to β-L-arabinopyranose units (Fernández et al., 2013), while the latter one corresponds to β-D-xylopyranose units. The major arabinose derivative detected between the partially methylated sugars in F1D is 2,3-di-*O*-methylarabinose, indicating that the arabinan backbone is constituted by 4-linked arabinopyranose units. Besides, the presence of 3-*O*-methylarabinose, suggests that part of these units are substituted on C2 with xylose. These results were confirmed by analysis of the whole NMR spectra, as follows (Fig. 1b): The other important signals in the HSQC spectrum are those at δ 69.3/3.88, 69.1/4.05, 75.2/3.98, and 60.4/4.02,3.75, which correspond to C2/H2-C5/H5,5' of 4-linked non-substituted β-L-arabinopyranose units, respectively. Those corresponding to C2/H2 and C3/H3 were assigned based on the correlation of the signals at δ 5.02 and 3.89 found on the COSY spectrum (Fig. 1c). Signals of C2/H2-C5/H5,5' of the single stubs of β-D-xylopyranose were assigned based on previously reported data (Cardoso, Noseda, Fujii, Zibetti, & Duarte, 2007; Usov & Elashvili, 1991). For these side chains, it has been shown that chemical shift of the anomeric carbon signal is greatly influenced by the place of substitution and by the backbone structure, but the other signals are almost independent of these structural features. Usually, substitution on one position, either with sulfate or with side chains, produces an upfield shift of the neighbouring carbons of 1–2 ppm (Usov, Yarotsky, & Shashkov, 1980). However, in some cases, the opposite effect is produced in the anomeric carbon signal, when substitution is on C2 (Ciancia, Matulewicz, Finch, & Cerezo, 1993). This effect is possibly due to conformational changes (Stortz & Cerezo, 1998). In this case, a small downfield shift of 0.7 ppm of C1 was observed by substitution of 4-linked β-L-arabinopyranose units with xylose. On the other hand, the expected shifts of C2/H2 and C3/H3 were observed, while the other C/H signals are overlapped with those of the major unsubstituted units of the backbone. Correlation at δ 5.18/4.00 in the COSY spectrum confirms the linkage position of the xylose side chains (Fig. 1c). NMR assignments are shown in Table 3.

Methylation analysis of F1D, did not allow to establish whether the galactose units are linked to C2 and/or C3 of the arabinose units of the arabinan backbone.

F1 was submited to partial acid hydrolysis in conditions previously reported not to remove the sulfate esters or pyranosic glycosidic linkages (Bilan et al., 2007). The partially hydrolyzed product, F1H, gave a molar ratio Ara:Xyl:Gal:sulfate of 1.0:0.1:0.1:1.1, showing an important increase in the sulfate ratio, due mostly to the decrease in the amount of galactose.

Methylation analysis of F1H (Table 2) gave 2-*O*-methylarabinose as major methylated derivative, which corresponds, at least in major amounts to 4-linked arabinopynose units sulfated on C3. The corresponding signals were dedused based on the spectrum of the desulfated sample, the expected effect of sulfation on this position (Ruiz-Contreras, Kamerling, Breg, & Vliegenthart, 1988) and results from the HSQC (Fig. 2a) and COSY spectra, where the corresponding correlations were very clear.

In addition, important amounts of non-methylated arabinose were detected between the partially methylated derivatives, indicating significant quantities of 2,3-disulfated arabinopyranose units. Sulfation on C2 should produce an upfield displacement of the anomeric carbon signal, as well as a downfield shift of the anomeric proton. Analysis of the HSQC spectrum of F1H showed a signal at δ

Table 1
Yields and analyses of CX2 and CC2 from *Cladophora falklandica*, and of the major products obtained by fractionation of CX2 by anion exchange chromatography on Sephadex A-25.[a]

Extract/Fraction	NaCl,M	Yield[b] %	Carbohydrates (anhydro) %	Sulfate (as SO_3Na) %	Monosaccharide composition moles%				
					Rha	Ara	Xyl	Gal	Glc
CX2	–	10.1	48.8	24.9	5.1	60.6	10.5	23.5	–
F1	–	46.5	51.9	17.5	4.6	56.3	13.4	22.3	3.4
F7	1.5	6.9	49.5	28.4	3.4	42.7	10.4	40.1	3.2
F8	2.0	6.4	26.6	20.1	3.6	48.4	10.9	37.0	–
CC2	–	2.2	43.9	18.9	3.8	32.6	7.8	48.0	7.8

[a] Eleven fractions were obtained, however, only those indicated here had significant yields.
[b] Yields of the extracts are given for 100 g of milled seaweed. 68.5% of CX2 was recovered from the column.

Table 2
Methylation analysis of extracts CX2 and CC2 from *Cladophora falklandica*, of fractions F1, F7, and F8, obtained anion exchange chromatography of CX2, and some of their derivatives (F1D and F1H, and CC2D).[a]

Monosaccharide[b]	Assignment[c]	CX2	F1	F1D	F1H	F7	F8	CC2[d]	CC2D[d]
2,4-Rha	→ 3) Rha*p* (1 →	–	4	2	–	–	–	–	–
4-Rha	→ 2,3) Rha*p* (1 →	2	2	1	3	–	2	–	–
2,3,4-Xyl	Xyl*p* (1 →	9	11	7	7	7	4	–	5
2,3-Xyl	nd[e]	1	–	3	1	1	1	1	3
Xyl	nd	1	2	1	2	3	3	1	1
2,3,4-Ara	Ara*p* (1 →	–	3	8	–	–	–	5	–
2,3-Ara	→ 4) Ara*p* (1 →	3	3	46	16	4	3	2	38
2,4-Ara	Ara*p* 3 S (1 →	–	–	–	5	–	2	–	–
2-Ara	→ 4) Ara*p* 3 S (1 →	26	24	7	32	32	26	27	7
3-Ara	→ 4) Ara*p* 2 S (1 →	9	4	18	8	9	7	6	15
Ara	→ 4) Ara*p* 2,3 S (1 →	25	29	3	20	21	22	22	10
2,3,5,6-Gal	Gal*f* (1 →	6	4	1	–	6	4	5	3
2,4,6-Gal	→ 3) Gal*p* (1 →	–	–	–	–	–	–	1	1
2,3,6-Gal	→ 5) Gal*f* (1 → and/or → 4) Gal*p* (1 →	7	5	–	2	6	3	6	4
2,3,5-Gal	→ 6) Gal*f* (1 →	5	2	–	–	6	3	6	1
2,3-Gal	→ 5,6) Gal*f* (1 → and/or → 4,6) Gal*p* (1 →	3	2	1	–	2	1	6	7
2,4-Gal	→ 3) Gal*p* 6 S (1 →	2	1	1	2	1	8	4	1
Gal	nd	3	3	2	2	3	11	6	3

[a] Moles% of the different monosaccharides derivatives.
[b] Monosaccharides having methyl groups at the positions indicated.
[c] S indicates substitution with sulfate groups or side chains.
[d] Significant quantities of 2,3,6-Glc, which derives from contamination with starch. This was confirmed by the presence of small peaks corresponding to 4-linked α-D-glucopyranose units in the NMR spectra of these samples.
[e] These derivatives were not assigned to a structural unit, and could derive from a small degree of undermethylation.

Table 3
Signal assignments (ppm) of NMR spectra of sulfated xylogalactoarabinans from *Cladophora falklandica*, and from their derivatives.

Structural unit	Chemical shifts, ppm[a,b]						Detected clearly in the spectrum of…[b]
	C-1/H-1	C-2/H-2	C-3/H-3	C-4/H-4	C-5/H-5,5′	C-6/H-6,6′	
4-linked α-L–Ara*p*	97.4/5.02	69.3/3.88	69.1/4.05	75.2/3.98	60.4/4.02,3.75		F1D
4-linked α-L –Ara*p* with β-D-Xyl*p* on C-2	98.1/5.18	78.8/4.00	67.9/4.14				F1D
T β- D-Xyl*p*	105.7/4.46	74.2/3.29	76.5/3.37	70.2/3.57	66.0/3.90,3.23		all
4-linked α-L–Ara*p* 3-sulfate	97.9/5.07	67.3/4.14	76.7/4.63	74.2/4.34	60.9/3.75, 3.80		F1H
4-linked α-L–Ara*p* 2,3-disulfate	96.7/5.34	75.5/4.64	73.6/4.70				F1H
T β- D-Gal*f*	108.8/4.98	82.0/4.04	77.7/3.97	84.5/3.96	71.6/3.75	63.7/3.58,3,65	F1, F7, F8, CC2
5-linked β- D-Gal*f*	108.9/5.21			82.9/4.14	77.2/4.16	62.0/3.74	F8, CC2des
6-linked β- D-Gal*f*	109.1/5.15			84.6/3.92	70.5/3.90	70.3/3.86,3.98	F1,F7, CC2des
Terminal non-reducing α-L –Ara*p* 3-sulfate		67.4/3.98	78.2/4.54	68.6/4.30	63.8/4.24,4.28		F1H
3-linked β- D-Gal*p* 6S	103.8/4.51	69.4/3.65	83.3/3.70	69.4/4.06	74.0/3.90	68.3/4.26	F7, F8
α/β-Rha*p*	102.8/4.61102.3/4.70					17.8/1.26 (d, 12 Hz)	F7, F8

[a] With reference to internal acetone at δ_{CH3} 31.2/2.15.
[b] Fraction where the unit was present in important amounts, bearing full assignment, diagnostic peaks were present in several spectra for each unit.

96.7/5.34, which was assigned to these units. Moreover, the signal at 5.34 correlates with that at 4.64, which correlates with that at 4.70 in the COSY spectrum. These correlations allowed us to assign C1/H1-C3/H3 of these units (Table 3). The other partially methylated arabinose derivatives correspond to 4-linked non-substituted arabinopyranose and to arabinopyranose units substituted on C2 with xylose.

Besides, small signals of terminal reducing ends were detected in the anomeric region at δ 97.8/4.52 and 93.7/5.21 ($J_{1,2}$ = 7.8 and 3.5, from the ^{1}H NMR spectrum), showing a slight degree of hydrolysis of pyranosic glycosidic linkages. Based on this result, the small amount of 2,4-di-*O*-methylarabinose found by methylation analysis of F1H was attributed to terminal non-reducing ends, sulfated on C3. Signals of C2H2-C5/5,5′of these units were present in the NMR

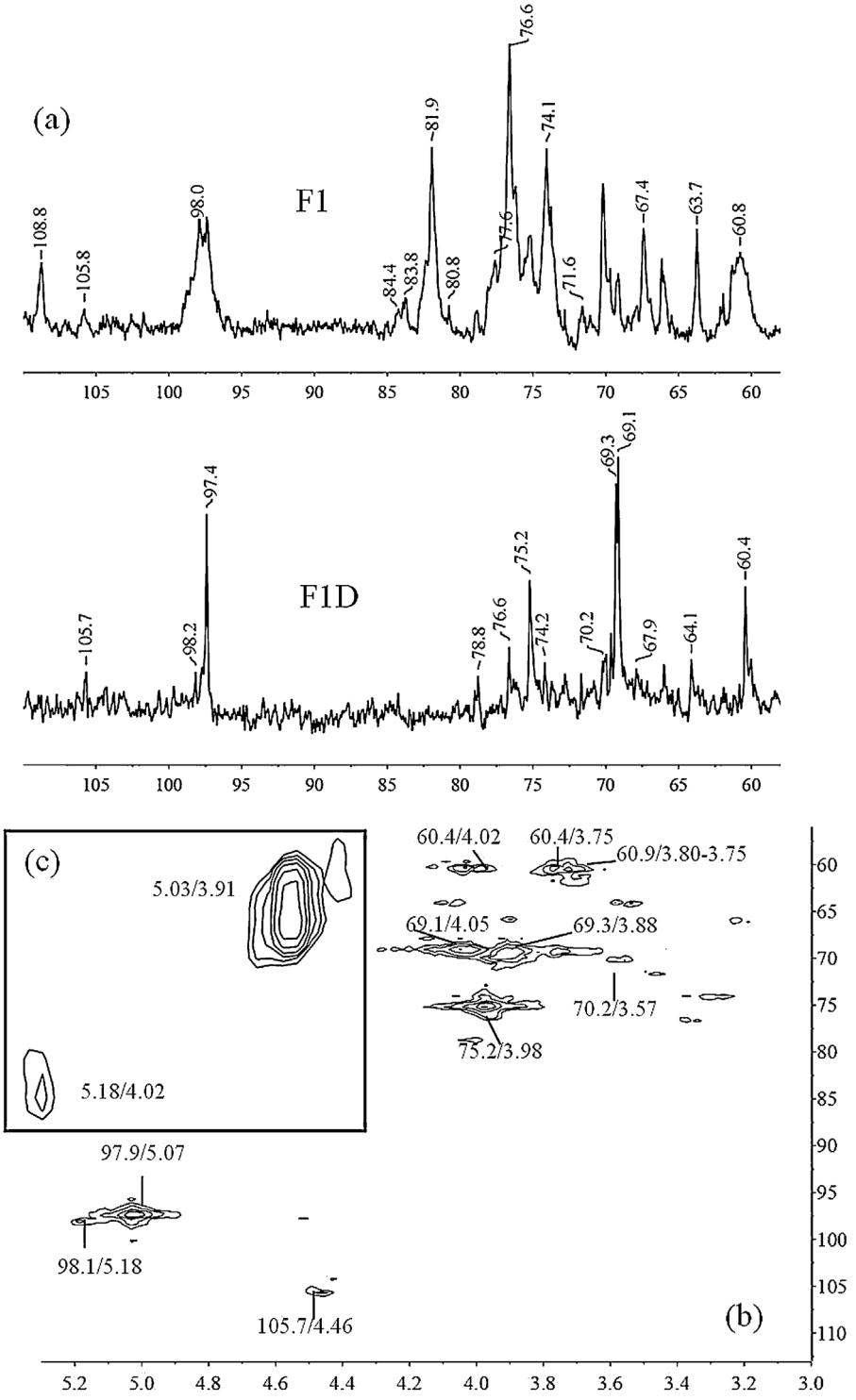

Fig. 1. (a) ^{13}C NMR spectra of F1 and F1D. (b) Full HSQC spectrum of F1D. (c) Detail of COSY spectrum of F1D, showing correlation between H1 and H2 of non-sulfated β-L-arabinopyranose units.

spectra, the anomeric signal should be overlapped with those of the major structures (Table 3) (Bock & Pedersen, 1982; Ruiz Contreras, Kamerling, Breg, & Vliegenthart, 1988).

Methylation analysis of F1 showed significant amounts of 2,3,5,6-tetra-*O*-methyl- and 2,3,5-tri-*O*-methy-galactose. It is important to emphasize that reductive hydrolysis was used in this study to obtain the corresponding alditol acetates from the per-methylated polysaccharides (Stevenson & Furneaux, 1991). This method was used because preliminary results obtained using the standard conditions for hydrolysis of the methylated sample (TFA 2 M 2 h at 120 °C, Morrison, 1988) and further reduction with $NaBH_4$, only gave traces of 2,3,5,6-tetra-*O*-methylgalactose (0.5%). On the other hand, 2,3,6-tri-*O*-methygalactose could derive either from 4-linked galactopyranose or 5-linked galactofuranose, or from both structural units. The fact that in the harder hydrolysis conditions described above, a part of this partially methylated

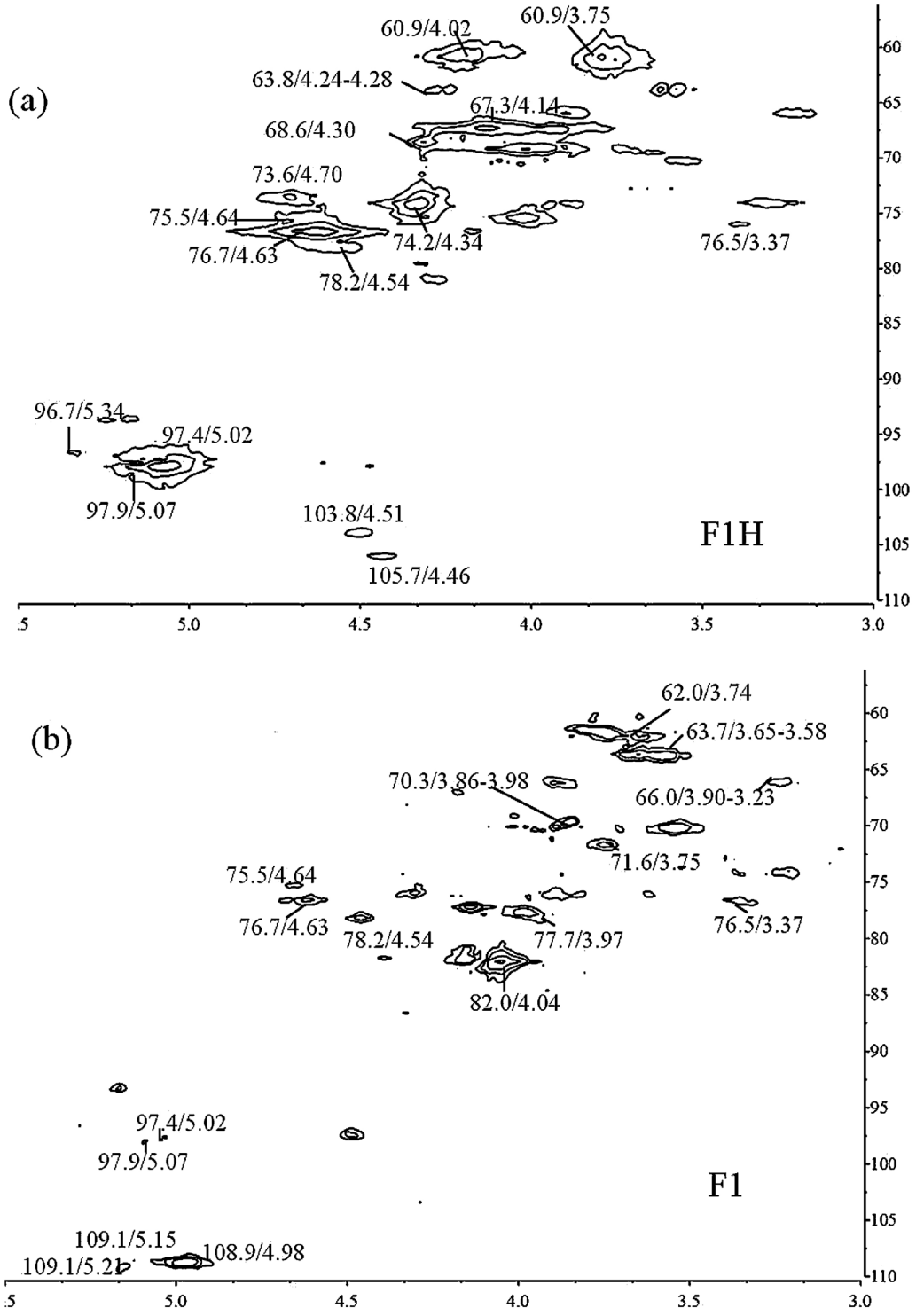

Fig. 2. HSQC spectra of F1H (a) and F1 (b).

derivative was lost, would indicate that indeed at least part of this partially methylated monosaccharide derives from furanosic galactose units. On the other hand, small amounts of 2,4-di-*O*-methygalactose, which corresponds to 3,6-linked galactopyranose units, were also present.

Regards arabinose units, methylation analyses of F1 and its derivatives show that the 4-linked disubstituted and monosubstituted on C3 are the only important substitution patterns, with sulfate groups or side chains, giving a highly substituted pyranosic arabinan.

Pyranosic arabinans have been previously isolated from green seaweeds of the genus *Codium* (Fernández et al., 2013; Fernández, Raffo, Alberghina, & Ciancia, 2015). However, these polysaccharides were 3-linked. The one obtained from *C. vermilara* was linear and highly sulfated, while that from *C. decorticatum* was less sulfated and with a certain degree of branching. On the other hand, 4-linked

pyranosic arabinose units, partially sulfated on C3 were reported for an arabinogalactan from green seaweed *Caulerpa racemosa* (Bryopsidales), which contained also 3-linked galactose, partially sulfated on C6, and terminal- and 4-linked xylopyranose (Chattopadhyay, Adhikari, Lerouge, & Ray, 2007).

Fig. 2b shows the HSQC spectrum of F1, where the predominant signals correspond to the β-D-galactofuranose units, which are present mostly as non reducing terminal residues. All the signals corresponding to these terminal units were assigned based on previous reports (Prieto et al., 1997; Prieto et al., 2001; Petersen, Meier, Smestad Paulsen, Redondo, & Skovsted, 2014) and signal correlations (Table 3). In the anomeric region there are two more signals at δ 109.1/5.21 and 109.1/5.15. Based on methylation analysis, they would derive from 5- or 6-linked units, but it was not possible to determine which of them corresponds to each of these residues. However, peaks of C4/H4, C5/H5, and C6/H6,6′ were assigned (see later). Besides, peaks corresponding to β-D-xylopyranose side chains were also clear. Although several efforts were done, as analysis of the HMBC spectrum of F1, it was not possible to determine with complete certainty the position of the linkage of galactofuranose units to the arabinan backbone. This is due to the complexity of the polysaccharide structure and to the similar chemical shifts of C2/H2 and C3/H3 of the non-substituted arabinan. In summary, Fig. 3 shows the structural features of the sulfated, highly ramified xylogalactoarabinan F1.

Polymers containing β-D-galactofuranose have not been detected in any other seaweed. However, they were found in some green microalgae species involved in mutualistic relationship with terrestrial fungi (lichens). These polysaccharides had usually a main backbone of β-D-galactofuranose units, with different side chains, comprising single stubs of β-D-galactofuranose and/or more complex branched structures, which comprise in some cases α-L-rhamnopyranose units (Cordeiro et al., 2005; Cordeiro et al., 2012; Cordeiro, Beilke, Reinhardt, Sassaki, & Iacomini, 2013). Moreover, in galactans from *Trebouxia* sp. a backbone of 5-linked β-D-galactofuranose units with single stubs of β-D-galactofuranose linked to C6, was reported (Cordeiro et al., 2005). On the other hand, β-D-galactofuranose is well known as constituent of infectious microorganisms of important biological significance, such as the bacteria, trypanosomatids, and fungi, but they are absent in plants and mammalian cells.

Methylation analyses (Table 2) and NMR spectra of F7 and F8 (Supplementary Fig. 1) were very similar to those of F1, in F8 a certain degree of submethylation was obtained, so these results should be considered with care. The HSQC spectrum of F8 gave only two major signals in the anomeric region corresponding to β-D-galactofuranose units at δ 109.0/5.21 and 108.9/4.99, the latter one corresponds to β-D-galactofuranose terminal units. This was confirmed due to the presence of all the peaks of this unit (Table 3). The other one was assigned to 5-linked β-D-galactofuranose units, based on the presence of signals at δ 77.2/4.16 and 62.0/3.74 (C5/H5 and C6/H6 of this unit) and the absence of the signals of C5/H5 and C6/H6 of the 6-linked units. Based on this evidence, it was possible to assign the corresponding signals in F1 (see above and Table 3).

An important difference found between the spectra of F7 and especially F8, with those of F1 was the presence of signals corresponding to 3-linked β-D-galactopyranose units sulfated on C6, in agreement with methylation analysis of this sample, which showed 8% of 2,4-di-*O*-methylgalactose between the partially methylated monosaccharides of F8. Whether this structure is part of the arabinan structure or a contaminant polysaccharide was not determined.

Besides, in the spectra of F7 and F8 a small peak at 17.8/1.26 (d, ~12 Hz) was assigned to C6/H6 of rhamnose units, the anomeric signals at δ 102.8/4.61 and 102.3/4.70 would correspond to these units (Supplementary Fig. 1). In agreement with this, small amounts of 3-linked and 2,3-linked rhamnose units were detected by methylation analysis of most the samples investigated here. Until now, it was not possible to determine if the rhamnose units derive from another polysaccharide, a rhamnan, possibly with common structural features with those found in other green seaweeds, like *Monostroma* (Li et al., 2011) and *Gayralia* sps. (Cassolato et al., 2008), or if they are part of the major polysaccharide structure.

3.3. Chemical characterization of the hot water extract CC2

Analysis of CC2 (Table 1) showed some differences in the monosaccharide composition regards CX2 and fractions obtained from it, namely, the predominance of galactose over arabinose, and a small amount of glucose. Besides, the degree of sulfation is slightly lower (ratio carbohydrates: sulfate 1:0.73, for CX2 and 1:0.61, for CC2).

The structural features of CC2 were investigated by methylation and desulfation-methylation analysis (Table 2), and by NMR spectroscopy of the parent sample and its desulfated derivative (Supplementary Fig. 2).

In this case, galactose was not lost in such important amounts during the desulfation procedure, as in F1. In agreement with this, the conversion to the pyridinium salt gave a solution of pH 5.0, which was neutralized immediately. Analysis of the methylation pattern of the arabinose units of CC2 and CC2D indicated that sulfation was predominantly on C3, and most of the side chains would be linked to C2. These results suggest that the galactose side chains are linked, at least in CC2, predominantly to C2. The NMR spectra of CC2 did not show anomeric signals of the arabinose units in the region at $\delta < 97$, indicating that substitution on C2 corresponds to side chains, not to sulfation. It is reasonable to think that substitution with side chains on C2 would cause similar effects on C1, either in the case of β-D-xylopyranose or β-D-galactofuranose, that is, a small displacement of the signal to lower fields. This is in agreement with results from methylation and desulfation-methylation analyses. Besides, in CC2 the galactofuranose units appear to be forming longer chains. The presence of significant amounts of 2,3-di-*O*-methylgalactose between the partially methylated derivatives obtained from CC2, which were also present in CC2D indicates the presence of 5,6-linked galactofuranose units, consequently, ramifications of the galactofuranose chains. No evidence of these side chains was found in the fractions obtained from CX2.

On the other hand, a small amount of β-D-galactopyranose units sulfated on C6 was detected in CC2, as found before in F8.

3.4. Anticoagulant activity of the xylogalactoarabinan F1

Anticoagulant activity of F1 was assessed by measuring the prothrombin time (PT), the activated partial thromboplastin time (APTT), and thrombin time (TT). No clotting inhibition was observed in PT test at the concentrations assayed. On the contrary, APTT and TT were statistically prolonged, in a concentration dependent manner, regards the control (Fig. 4a and b). TT increases were higher than those observed in APTT. The APTT measures activity of the intrinsic and common pathways of coagulation, meanwhile the increase of TT indicates either thrombin inhibition (direct or mediated by AT and/or HCII) or impaired fibrin polymerization. Moreover, prolongation of the TT-like assay, using fibrinogen (3 mg/mL) instead of plasma, was also observed when F1 (100 μg/mL) was pre-incubated with the fibrinogen for 30 min and then thrombin was added in the same way as in the TT assay. The ratio for F1 was 2.5 ± 0.2. This is a first signal of a possible direct inhibition of F1 on thrombin activity, taking into account that AT and HCII were absent in the test. However, more studies need to be done to confirm this hypothesis. Our results demonstrate that F1 exerts anticoagulant effect, although, when compared to model

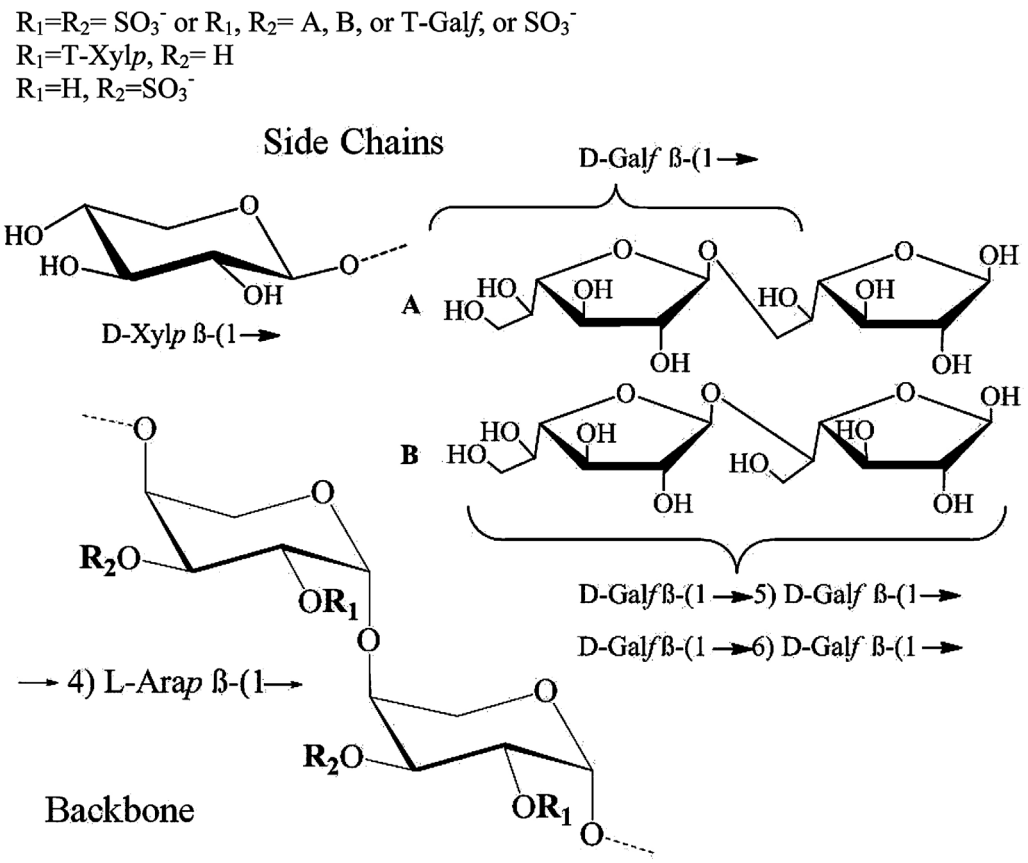

Fig. 3. Structure of xylogalactoarabinan F1 from *Cladophora falklandica*.

anticoagulants, such as heparin and dermatan sulfate, F1 proved to be less potent in preventing *in vitro* clot formation.

3.5. Studies of fibrin formation and fibrinolysis

3.5.1. Fibrin formation kinetics

All the assayed concentrations of F1 produced statistically significant changes in kinetic parameters. Thus, F1 caused a decreased fibrin formation rate and OD_{Max} regards the control in a concentration dependent manner (Fig. 4c). No plasma coagulation was detected using more than 50 μg/mL of the polysaccharide. Moreover, when solutions of F1 were assayed on purified system, *i.e.* on purified fibrinogen, changes in the kinetic parameters of F1 *vs.* control were still observed. In particular, using 15 μg/mL a decrease in the *slope* (4.0 ± 1.4 min vs. 14.0 ± 2.8 min), an increase in the *lag phase* (3.4 ± 0.5 min vs. 0.0 ± 0.0 min) and a decrease in the OD_{Max} (0.171 ± 0.008 vs. 0.360 ± 0.004) were observed (Supplementary Fig. 3). Besides the TT-like assay, this test is another way to demonstrate that F1 induces changes directly on thrombin and/or fibrinogen.

3.5.2. Analysis of fibrin networks by SEM

Among all the concentrations tested those that allowed clot formation and further processing of the clot for analysis by SEM were chosen. Fig. 4d shows the electronic microscopy images of the fibrin network obtained from plasma incubated with F1 at the minimum concentration that showed significant differences (15 μg/mL), and from a control network with saline solution. Quantitative analysis of the photographs showed statistically different fibrin networks structure between sample and control. The network percentage (50.5 ± 5.1) and the number of fibers per field (29.1 ± 5.8) were statistically significantly lower in fibrin in the presence of F1 than in the control (77 ± 2.1; 67.9 ± 3.9 respectively). In presence of the polysaccharide, a more opened network, with less cross-linking between fibers. In addition, results expressed as median (range) showed that the widths of the fibers were 0.158 (0.085–0.313) μm *vs.* 0.118 (0.062–0.236) μm and the fiber length 2.000 (0.439–4.756) μm *vs.* 1.162 (0.103–4.709) μm, respectively, indicating significantly thicker and longer fibers in the presence of F1 than those of the control.

3.5.3. Lysability assays

The plasma fibrin networks produced in the presence of F1 (15 μg/mL) were lysed by t-PA. The dissolution of the clots by the generated plasmin was reflected in the changes of the turbidity at 405 nm. Our results indicate that F1 generated a decrease of the *half-lysis-time* ($t_{1/2}$, 18.0 ± 3.6 min vs. 29.3 ± 2.9 min).

Structural properties of fibrin are related to clot stability, which in turn depends on the resistance to mechanical stress and fibrinolytic dissolution. Contradictory results were reported. On one hand, it has been described that plasma fibrin clots with dense fiber arrangements made of thin strands, dissolve at a slower rate than those with a coarse fibrin structure made of thicker fibers (Meh et al., 2001; Weisel, 2007). On the contrary, it was reported (Collet et al., 2000; Wu, Siddiqui, & Diamond, 1994) that thicker fibers were lysed more slowly than thinner ones, while other authors showed that the cleavage rate of thin and thick fiber networks were the same. Nevertheless, it was found that the major factor determining the fibrinolysis rate is the meshwork configuration, rather than fiber diameter (Collet, Lesty, Montalescot, & Weisel, 2003), likely because of a less efficient transport of fibrinolytic agents through the fibrin clot (Carr & Alving, 1995; Kolev & Machovich, 2003). In

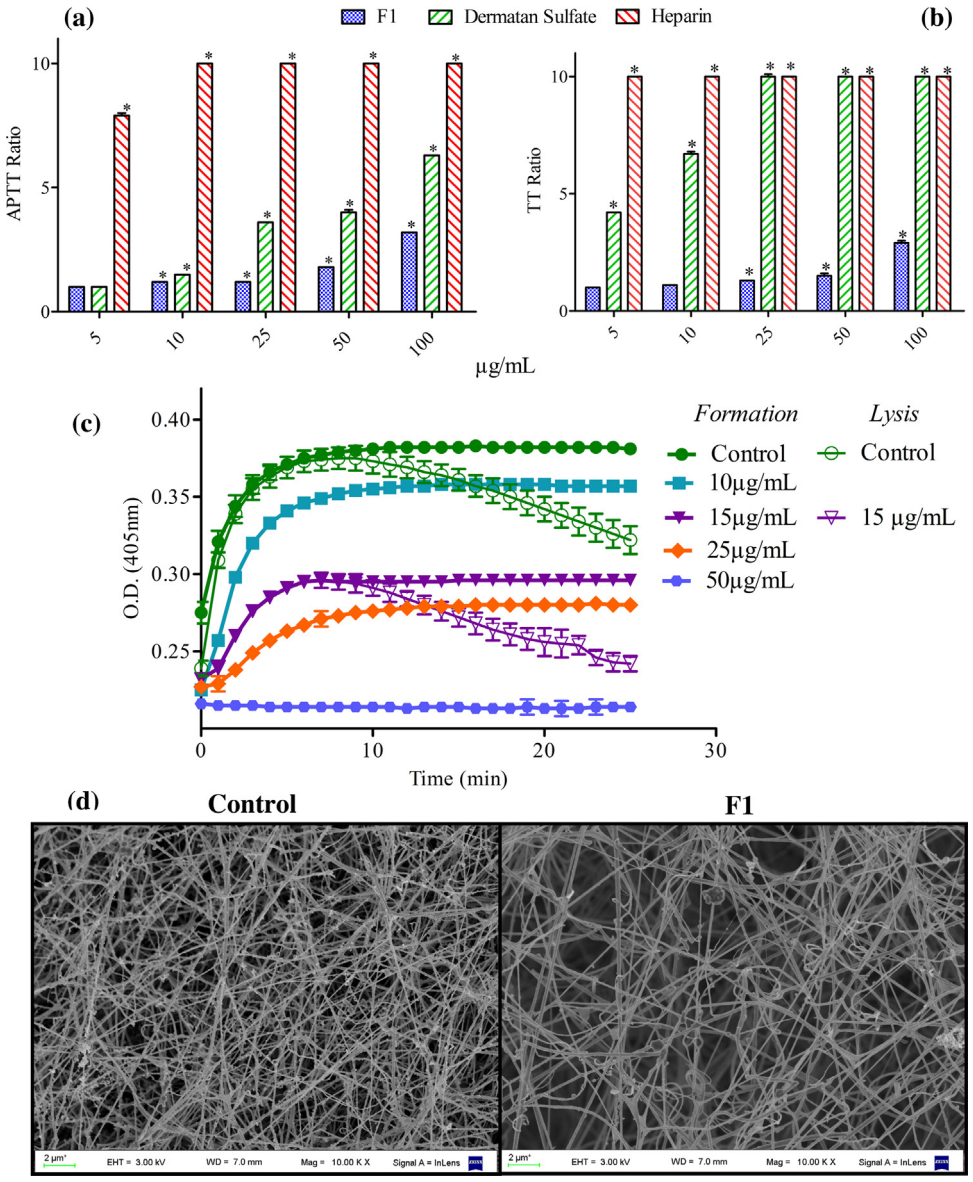

Fig. 4. Activated partial thromboplastin time (APTT) (a) and Thrombin time (TT) (b) of fraction F1 from *Cladophora falklandica*, dermatan sulfate and heparin. Effects of F1 on the kinetics of fibrinformation and fibrinolysis (c). Fibrin structure by SEM of F1 compared with the control (d).
*Student's *t*-test was used to compare the curveís parameters, *Fibrin formation kinetic*, Curves represent the average of $OD_{(450nm)}$ (n = 4) versus time for each sample * Statistically significant differences ($p < 0.05$), Bars indicate the size reference (µm).

accordance with the latest assumption, our results showed that in the presence of F1, the more opened network obtained rendered a faster fibrinolysis, although the network had thicker fibers than control.

Sulfated polysaccharides occur in high amounts in marine algae. However, their therapeutic use in humans faces several challenges. It is crucial to find an alternative approach in order to establish a new paradigm, instead of looking at them as "heparin-like molecules" (Mourão, 2015).

4. Conclusions

The major water-soluble polysaccharides from *Cladophora falklandica* are sulfated xylogalactoarabinans. Their backbone is constituted by 4-linked pyranosic β-L-arabinose units. 3-Linked sulfated pyranosic arabinans were previously isolated from *Codium* species (Bryopsidales). On the other hand, pyranosic arabinose units were found to be part of arabinogalactans from green seaweeds *Caulerpa racemosa* (Bryopsidales) and *Cladophora rupestris*; however, their structure was not fully determined. In addition, the water-soluble polysaccharides from the latter seaweed comprised galactose units in the furanosic form. In this paper, it was found that for the arabinan of *Cladophora falklandica*, these units constitute side chains of the backbone. As far as we know, this is the only case, in which the presence of galactofuranose was proved for seaweed polysaccharides, and their structure was determined. These results show that the presence of sulfated pyranosic arabinans is characteristic of algae of the Cladophorales and Bryopsidales, but similar polymers were not found in other important orders of green algae. In addition, these arabinans showed galactofuranose units. The extent of the generalization of this structural characteristic in the Cladophorales is still not known.

In the presence of F1 the coagulation process slower. One of the possible mechanisms of the anticoagulant effect of F1 is direct thrombin inhibition. Our previous results with other sulfated polysaccharides from green seaweeds showed that direct thrombin inhibition was also one of the mechanisms involved in the inhibition of coagulation. F1 modified the kinetics of fibrin formation suggesting an impaired polymerization process. SEM showed a laxer conformation of the fibrin network, with large interstitial pores as compared with control fibrin architecture. Accordingly, these networks proved to be lysed more easily.

For haemostasis to be efficient, there must be equilibrium between clotting and lysis: the plug should be formed, but it must be removed, so as not to cause thrombosis. F1 could be a modulator of fibrin properties by rendering clots more susceptible to lysis, reducing the permanence in the blood vessel and, consequently, generating a lesser thrombogenic state. Hence, this xylogalctoarabinan from the green seaweed *Cladophora falklandica* deserves to be investigated as potential anticoagulant.

Acknowledgement

This work was supported by a grant from the University of Buenos Aires, UBACYT 2014–2017, 20020130100576BA.

Appendix A. Supplementary data

Supplementary data associated with this article can be found, in the online version, at http://dx.doi.org/10.1016/j.carbpol.2016.07.088.

References

Anand, S., Yusuf, S., Pogue, J., Ginsberg, J., & Hirsh, J. (2003). Relationship of activated partial thromboplastin time to coronary events and bleeding in patients with acute coronary syndromes who receive heparin. *Circulation*, *107*, 2884–2888.

Angell, A. R., Mata, L., de Nys, R., & Paul, N. A. (2016). The protein content of seaweeds: A universal nitrogen-to-protein conversion factor of five. *Journal of Applied Phycollogy*, *28*, 511–524.

Arata, P. X., Quintana, I., Canelón, D. J., Vera, B. E., Compagnone, R. S., & Ciancia, M. (2015). Chemical structure and anticoagulant activity of highly pyruvylated sulfated galactans from tropical green seaweeds of the order Bryopsidales. *Carbohydrate Polymers*, *122*, 376–386.

Bilan, M. I., Vinogradova, E. V., Shashkov, A. S., & Usov, A. I. (2007). Structure of a highly pyruvylated galactan sulfate from the pacific green alga *Codium yezoense* (Bryopsidales, Chlorophyta). *Carbohydrate Research*, *342*, 586–596.

Bock, K., & Pedersen, C. (1982). Carbon-13 nuclear magnetic resonance spectroscopy of monosaccharides. *Advances in Carbohydrate Chemistry and Biochemistry*, *41*, 27–66.

Bradford, M. M. (1976). A rapid and sensitive method for the quantitation of microgram quantities of protein utilizing the principle of protein dye binding. *Analytical Biochemistry*, *72*, 248–254.

Cardoso, M. A., Noseda, M. D., Fujii, M. T., Zibetti, R. G., & Duarte, M. E. (2007). Sulfated xylomannans isolated from red seaweeds *Chondrophycus papillosus* and *C. flagelliferus* (Ceramiales) from Brazil. *Carbohydrate Research*, *342*, 2766–2775.

Carr, M. E., & Alving, B. M. (1995). Effect of fibrin structure on plasmin-mediated dissolution of plasma clots. *Blood Coagulation and Fibrinolysis*, *6*, 567–573.

Cases, M. R., Cerezo, A. S., & Stortz, C. A. (1995). Separation and quantitation of enantiomeric galactoses and their mono-*O*-methylethers as their diastereomeric acetylated 1-deoxy-1-(2-hydroxypropylamino) alditols. *Carbohydrate Research*, *269*, 333–341.

Cassolato, J. E. F., Noseda, M. D., Pujol, C. A., Pellizzari, F. M., Damonte, E. B., & Duarte, M. A. R. (2008). Chemical structure and antiviral activity of the sulfated heterorhamnan isolated from the green seaweed *Gayralia oxysperma*. *Carbohydrate Research*, *343*, 3085–3095.

Chattopadhyay, K., Adhikari, U., Lerouge, P., & Ray, B. (2007). Polysaccharides from *Caulerpa racemosa*. Purification and structural features. *Carbohydrate Polymers*, *68*, 407–415.

Ciancia, M., Matulewicz, M. C., Finch, P., & Cerezo, A. S. (1993). Determination of the structures of cystocarpic carrageenans from *Gigurtina skottsbergii* by methylation analysis and NMR spectroscopy. *Carbohydrate Research*, *238*, 241–248.

Ciancia, M., Quintana, I., Vizcargüénaga, M. I., Kasulin, L., de Dios, A., Estevez, J. M., et al. (2007). Polysaccharides from the green seaweeds *Codium fragile* and *C. vermilara* with controversial effects on hemostasis. *International Journal of Biological Macromolecules*, *41*, 641–649.

Ciancia, M., Quintana, I., & Cerezo, A. S. (2010). Overview of anticoagulant activity of sulfated polysaccharides from seaweeds in relation to their structures, focusing on those of green seaweeds. *Current Medicinal Chemistry*, *17*, 2503–2529.

Ciucanu, I., & Kerek, K. (1984). A simple and rapid method for the permethylation of carbohydrates. *Carbohydrate Research*, *134*, 209–217.

Collet, J. P., Park, D., Lesty, C., Soria, J., Soria, C., Montalescot, G., et al. (2000). Influence of fibrin network conformation and fibrin fiber diameter on fibrinolysis speed: Dynamic and structural approaches by confocal microscopy. *Arteriosclerosis Thrombosis and Vascular Biology*, *20*, 1354–1361.

Collet, J. P., Lesty, C., Montalescot, G., & Weisel, J. W. (2003). Dynamic changes of fibrin architecture during fibrin formation and intrinsic fibrinolysis of fibrin-rich clots. *Journal of Biological Chemistry*, *278*, 21331–21335.

Cordeiro, L. M. C., Carbonero, E. R., Sassaki, G. L., Reis, R. A., Stocker-Wörgötter, E., Gorin, P. A. J., et al. (2005). A fungus-type β-galactofuranan in the cultivated *Trebouxia* photobiont of the lichen *Ramalina gracilis*. *FEMS Microbiology Letters*, *244*, 193–198.

Cordeiro, L. M. C., Beilke, F., Bettim, F. L., Reinhardt, V. F., Rattmann, Y. D., & Iacomini, M. (2012). (1 → 2) and (1 → 6)-linked β-D-galactofuranan of microalga *Myrmecia biatorellae*: Symbiotic partner of *Lobaria linita*. *Carbohydrate Polymers*, *90*, 1779–1785.

Cordeiro, L. M. C., Beilke, F., Reinhardt, V. F., Sassaki, G. L., & Iacomini, M. (2013). Rhamnogalactofuranan from the microalga *Myrmecia biatorellae*: Symbiotic partner of *Lobaria linita*. *Phytochemistry*, *94*, 254–259.

Dodgson, K. S., & Price, R. G. (1962). A note on the determination of the ester sulphate content of sulphated polysaccharides. *Biochemistry Journal*, *84*, 106–110.

Dubois, M., Gilles, K. A., Hamilton, J. K., Rebers, P. A., & Smith, F. (1956). Colorimetric method of determination of sugars and related substances. *Analytical Chemistry*, *28*, 350–356.

Fernández, P. V., Quintana, I., Cerezo, A. S., Caramelo, J. J., Pol-Fachin, L., Verli, H., et al. (2013). Anticoagulant activity of a unique sulphated pyranosic (1(3)-β-L-arabinan through direct interaction with thrombin. *Journal of Biological Chemistry*, *288*, 223–233.

Fernández, P. V., Raffo, M. P., Alberghina, J., & Ciancia, M. (2015). Polysaccharides from the green seaweed *Codium decorticatum*: Structure and cell wall distribution. *Carbohydrate Polymers*, *117*, 836–844.

Filisetti-Cozzi, T. M., & Carpita, N. C. (1991). Measurement of uronic acids without interference from neutral sugars. *Analytical Biochemistry*, *197*, 157–162.

Kelton, J. G., & Hirsh, J. (1980). Bleeding associated with antithrombotic therapy. *Seminars Hematology*, *17*, 259–291.

Kelton, J. G., & Warkentin, T. E. (2008). Heparin-induced thrombocytopenia: A historical perspective. *Blood*, *112*, 2607–2616.

Koepsell, H. J., & Sharpe, E. S. (1952). Microdetermination of pyruvic and α-ketoglutaric acids. *Archives of Biochemistry and Biophysics*, *38*, 443–449.

Kolev, K., & Machovich, R. (2003). Molecular and cellular modulation of fibrinolysis. *Thrombosis and Haemostasis*, *89*, 610–621.

Laffan, M. A., & Bradshaw, A. E. (1995). Investigation of haemostasis. Practical haematology. In J. V. Dacie, & S. M. Lewis (Eds.), (pp. 297–315). New York: Churchill Livingstone.

Li, H., Mao, W., Zhang, X., Qi, X., Chen, Y., Chen, Y., et al. (2011). Structural characterization of an anticoagulant-active sulfated polysaccharide isolated from green alga *Monostroma latissimum*. *Carbohydrate Polymers*, *85*, 394–400.

Lowry, O. H., Rosenbrough, N. J., & Farr, A. L. (1951). Protein measurements with the Folin phenol reagent. *Journal of Biological Chemistry*, *193*, 265–275.

Meh, D. A., Mosesson, M. W., DiOrio, J. P., Siebenlist, K. R., Hernandez, I., Amrani, D. L., et al. (2001). Disintegration and reorganization of fibrin networks during tissue-type plasminogen activator-induced clot lysis. *Blood Coagulation Fibrinolysis*, *12*, 627–637.

Morrison, I. M. (1988). Hydrolysis of plant cell walls with trifluoroacetic acid. *Phytochemistry*, *27*, 1097–1100.

Mourão, P. A. S. (2015). Perspective on the use of sulfated polysaccharides from marine organisms as a source of new antithrombotic drugs. *Marine Drugs*, *13*(5), 2770–2784.

Navarro, D. A., Flores, M. L., & Stortz, C. A. (2007). Microwave-assisted desulfation of sulfated polysaccharides. *Carbohydrate Polymers*, *69*, 742–747.

Park, J. T., & Johnson, M. J. (1949). A submicrodetermination of glucose. *Journal of Biological Chemistry*, *181*, 149–151.

Percival, E., & McDowell, R. H. (1981). Algal walls: Composition and biosynthesis. In W. Tanner, & F. A. Loewus (Eds.), *Encyclopedia of plant physiology* (vol. 13B) (pp. 277–316). Berlin: Springer.

Petersen, B. O., Meier, S., Smestad Paulsen, B., Redondo, A. R., & Skovsted, I. C. (2014). Determination of native capsular polysaccharide structures of *Streptococcus pneumoniae* serotypes 39, 42, and 47F and comparison to genetically or serologically related strains. *Carbohydrate Research*, *395*, 38–46.

Prieto, A., Leal, J. A., Poveda, A., Jiménez-Barbero, J., Gómez-Miranda, B., Domenech, J., et al. (1997). Structure of complex cell wall polysaccharides isolated from *Trichoderma* and *Hypocrea* species. *Carbohydrate Research*, *304*, 281–291.

Prieto, A., Leal, J. A., Gómez-Miranda, B., Ahrazem, O., Jiménez-Barbero, J., & Bernabé, M. (2001). Structure of a cell wall polysaccharide isolated from *Hypocrea gelatinosa*. *Carbohydrate Research*, *333*, 173–178.

Quick, J. (1935). The prothrombin time in haemophilia and in obstructive jaundice. *Journal of Biological Chemistry*, *109*, 73–74.

Ruiz Contreras, R., Kamerling, J. P., Breg, J., & Vliegenthart, F. G. (1988). ^{1}H- and ^{13}C-n.m.r. spectroscopy of synthetic monosulphated methyl α-D-galactopyranosides. *Carbohydrate Research*, *179*, 411–418.
Sri Ramana, K., & Venkata Rao, E. (1991). Structural features of the sulphated polysaccharide from a green seaweed, *Cladophora socialis*. *Phytochemistry*, *30*, 259–262.
Stevenson, T. T., & Furneaux, R. H. (1991). Chemical methods for the analysis of sulphated galactans from red algae. *Carbohydrate Research*, *210*, 277–298.
Stortz, C. A., & Cerezo, A. S. (1998). Conformational analysis of sulfated α-(1 → 3)-linked D-galactobioses using the MM3 force-field. *Journal of Carbohydrate Chemistry*, *17*, 1405–1419.
Usov, A. I., & Elashvili, M. Y. (1991). Polysaccharides of algae 44. Investigation of sulfated galactan from *Laurencia nipponica* Yamada (Rhodophyta, Rhodomelaceae) using partial reductive hydrolysis. *Botanica Marina*, *34*, 553–560.
Usov, A. I., Yarotsky, S. V., & Shashkov, A. S. (1980). ^{13}C nmr spectroscopy of red algal galactans. *Biopolymers*, *19*, 977–990.
Weisel, J. W. (2007). Structure of fibrin: Impact on clot stability. *Journal of Thrombosis and Haemostasis*, *5*(Suppl. 1), 116–124.
Wissel, H., Mayr, C., & Lücke, A. (2008). A new approach for the isolation of cellulose from aquatic plant tissue and freshwater sediments for stable isotope analysis. *Organic Geochemistry*, *3*, 1545–1561.
Wolberg, A. S., Gabriel, D. A., & Hoffman, M. (2002). Analyzing fibrin clot structure using a microplate reader. *Blood Coagulation and Fibrinolysis*, *13*, 533–539.
Wu, J. H., Siddiqui, K., & Diamond, S. L. (1994). Transport phenomena and clot dissolving therapy: An experimental investigation of diffusion-controlled and permeation-enhanced fibrinolysis. *Thrombosis and Haemostasis*, *72*, 105–112.